A wide depth of field reconstruction method based on partially focused image series

Marcin Denkowski[*], Michał Chlebiej, Paweł Mikołajczak

Laboratory of Information Technology, Institute of Computer Science, Maria Curie Skłodowska University, Pl. M. Curie-Skłodowskiej 1, 20-031 Lublin, Poland

Abstract

The main problem with images acquired using macro photography is the very shallow depth-of-field. In this article we present and implement an algorithm to reconstruct full focused images based on partially focused images series of the same object acquired with different focus depths. The presented algorithm consists of several phases including: image registration, depth map creation, image reconstruction and final histogram and quality correction.

1. Macro Photography

Macro photography is a type of close-up photography. In the classical definition it is described as photography in which the image on film or electronic sensor is at least as large as the subject. Therefore, on 35mm film, the camera has to have the ability to focus on an area at least as small as 24×36 mm, equivalent to the image size on film (magnification 1:1). In other words, macro photography means photographing objects at extreme close-ups with magnification ratios from about 1:1 to about 10:1 (See Fig. 1 for photo example with such a magnification ratio). There are some primary difficulties in macro photography; one of the most crucial is the problem of insufficient lighting.

When using some cameras to take photos in the macro-mode, the camera must be positioned so close to the object that it touches the front piece of glass in the lens. In this case it is impossible to place a light source between the camera and the subject, making extreme close-up photography impractical. 50 mm is a typical focal-length lens used on a 35 mm camera, and can focus so close that the lighting problem remains. The method of choice in such situations is usually to use a telephoto macro lenses. When using such devices in macro photography it is possible to increase the focal length from 100 to 200mm.

---

[*]Corresponding author: *e-mail address*: denmar@goblin.umcs.lublin.pl

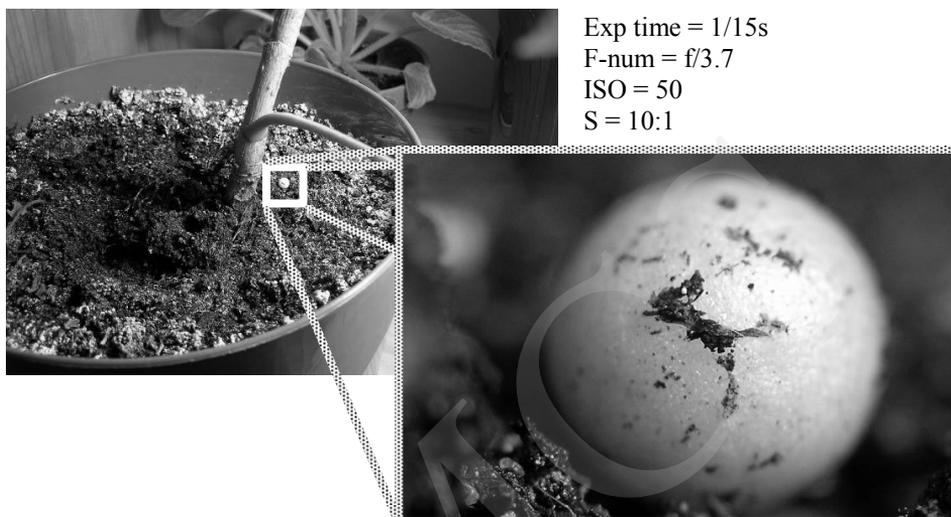Exp time = 1/15s
F-num = f/3.7
ISO = 50
S = 10:1

Fig. 1. Close-up of polystyrene ball, an example of macro photograph

The most crucial parameter of macro photography is the depth of field (DOF). Because it is very difficult to obtain high values of DOF for extreme close-ups it is essential to focus on the most important part of the subject. Any other elements that are even a millimeter farther or closer may appear blurred in the acquired photo. For this reason, special devices like advanced tripods for a medium-scale objects or microscope stage for micro-scale objects are required for precise focusing. The depth of field can be defined as the distance in front of and behind the subject appearing in focus. Only a very short range of the photographed subject will appear in exact focus. This focus decreases rapidly on either side of this distance, but due to imperfections of the human eye the focused area seems to be much bigger. This focused area decreases more quickly in front of the focus point than behind as the angle of the light rays changes more rapidly when it is closer to the lens, while becoming parallel with increasing distance. It is for these reasons that there is no precise definition of what is focused; there are many factors that determine whether the subject appears in focus. The most important factor is how a single point is mapped onto the film area. If a given point is exactly at the focus distance it will be imaged as one point on the film, but if this point is farther or nearer it will produce a disk whose border is known as a "circle of confusion". These circles can be used to define the measure of focus and blurriness as they increase in diameter the further away they are from the focus point. For the most common size of 35mm camera negative (22×16mm), the acceptable "circle of confusion" diameter at which human eye is able to distinguish such a circle as a dot is usually set to 0.05mm. The film size is also important when considering the depth of field problem because, for a given scene, the larger the negative is then the longer the

lens needed to capture it. Summarizing, for a specific film format, the depth of field is described as a function parameterized by: the focal length of the lens, the diameter of the lens opening (the aperture), and the distance between the subject and the camera.
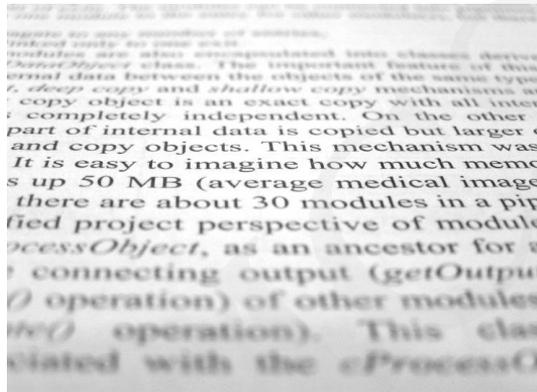

Fig. 2. An example of very shallow depth of field in a macro photograph

Let D be the distance at which the camera is focused, F the focal length (in millimeters) calculated for an aperture number f and k - the "circle of confusion" for a given film format (in millimeters), then depth of field (DOF) [1] can be defined as:

$$DOF_{1,2} = \frac{D}{1 \pm \dfrac{1000 \times D \times k \times f}{F^2}}, \tag{1}$$

where DOF_1 is the distance from the camera to the far depth of field limit, and DOF_2 is the distance from the camera to the near depth of field limit. As equation (1) shows, there are three main factors controlling the depth-of-field for a given film format. The aperture controls the effective diameter of the lens opening. Reducing the aperture size increases the depth of field, however, it also reduces the amount of light transmitted (see Figure 3).
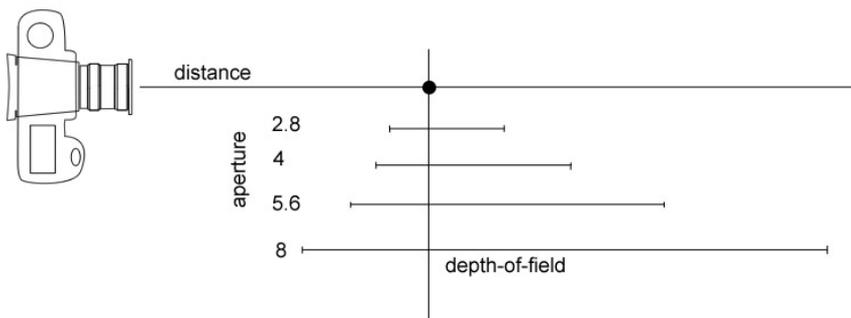

Fig. 3. Example diagram of how the f-number (aperture) affects depth-of-field

Lenses with a short focal length have a greater depth-of-field than long lenses. Greater camera-to-subject distance results in a greater depth-of-field.

2. Problem formulation and assumptions

In the previous paper we discussed what a macro photography is and we also presented its shallow depth-of-field problem. Our goal is to achieve the deepest possible depth-of-field using standard digital camera images and image processing algorithms. To achieve this we create a series of macro photograph images of the same subject with different focus lengths. The next step is to register them together. Following this we create a depth map using standard image processing algorithms. In the last step we reconstruct the focused image with a very deep depth-of-field using a generated depth map.

2.1. Image alignment algorithm

In the first step of the presented reconstruction method a set of photographs of the desired object is acquired. In the ideal case we can assume that the camera remains still during the acquisition process, which means that the images should be perfectly aligned. Unfortunately, in practice this is rarely the case. During extreme close-up sessions small movements of the camera are possible even when using tripods for stabilization. In some cases it is not possible to use any stabilization device. In such situations it is impossible to avoid camera movements. To make the reconstruction method more robust we can make use of an image registration procedure. The main idea behind image registration is to find perfect geometric alignment between a set of overlapping images. The quality of match measure represents the matching function parameterized by the geometric transformation. In our method we use the rigid (translations and rotation) or the affine transformation model (rigid + scaling and shears). In most cases it is sufficient to use the simplified rigid transformation (translations only). But when images are acquired without stabilization devices the use of complete affine transformation is a necessity. In our approach we use the normalized mutual information [3] as the matching function:

$$NMI(FI, RI) = \frac{h(FI) + h(RI)}{h(FI, RI)}, \tag{2}$$

where *RI* represents the reference image and *FI* represents the floating image.

$$h(FI) = -\sum p_{FI}(x) \log(p_{FI}(x)),$$
$$h(RI) = -\sum p_{RI}(x) \log(p_{RI}(x)), \tag{3}$$
$$h(FI, RI) = -\sum \sum p_{FI,RI}(x, y) \log(p_{FI,RI}(x, y)),$$

where $h(FI)$, $h(RI)$ and $h(FI,RI)$ are the single and joint entropies [2], p_{FI} and p_{RI} are the probabilities of each intensity in the intersection volume of both data sets

and $p_{FI,RI}$ is a probability distribution of a scatter-plot histogram. For the minimization of the selected similarity measure we use Powell's [4] algorithm. As a result of the registration procedures we obtain a set of geometrically matched images that can be used in the next stages of our wide depth of field reconstruction algorithm.

2.2. Image sharpening algorithm

The image-sharpening algorithm consists of several steps (see Figure 4). First we apply a standard Gaussian convolution filter to all images to produce blurry images. The Gaussian blur is a type of filter that uses a normal distribution for calculating the transformation we need to apply to every pixel in the image. The equation of Gaussian distribution is [5]:

$$f(r) = \frac{1}{\sqrt{2\pi}\sigma} \exp\left(\frac{-(r^2)}{2\sigma^2}\right), \tag{4}$$

where r is the blur radius ($r^2 = u^2 + v^2$), and σ is the standard deviation of the Gaussian distribution. Pixels that are non-zero for this distribution are used to build a convolution matrix, which is applied to the original image. Each pixel value is set to the weighted average for its neighborhood (see equation 5). The original pixel value receives the highest weight (having the highest Gaussian value), and neighboring pixels receive progressively smaller weights as their distance to the original pixel increases. This results in a blur that preserves boundaries and edges better than other, more uniform blurring filters.

$$g(x,y) = \sum_{s=-r}^{r} \sum_{t=-r}^{r} w(s,t) \cdot f(x+s,y+t), \tag{5}$$

where $w(s,t)$ is convolution matrix value at (s,t) coordinates, $f(x+s, y+t)$ is the image pixel value at (x+s, y+t) coordinates.

Fig. 4. An example of a Gaussian blur filtering; Image on the right was created by applying a Gaussian blur filter ($\sigma = 2$ and r=6) to the image on the left
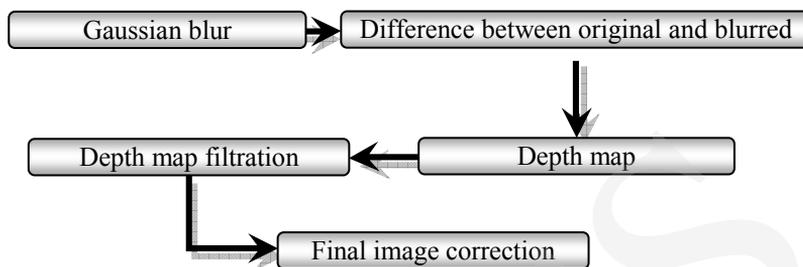
Fig. 5. Image sharpening algorithm diagram

These blurred images are subtracted from theirs originals, i.e. each pixel value is set to an absolute difference between the blur pixel and the pixel taken from the original image, according to this equation:

$$f_r(x,y) = \left| f_{org}(x,y) - f_{blur}(x,y) \right|. \tag{6}$$

An example of original images and their difference images $f_r(x,y)$ are shown in Figure 6.
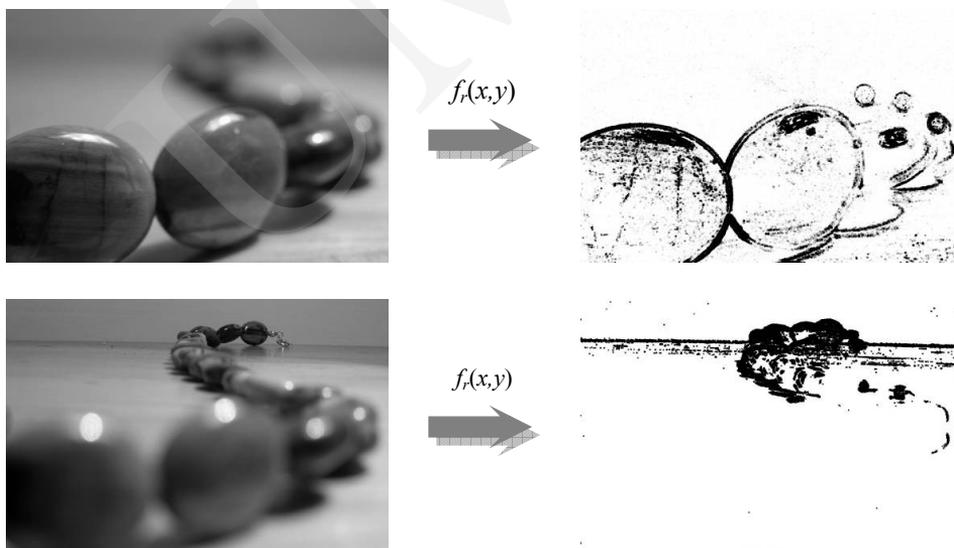

Fig. 6. Original image (on the left) and the image created through subtraction of the original image and the blurred image according to eq. (6) (on the right, here is a thresholded negative of that image)

In the next step we create the depth map. For this purpose, the global minimum *gmin* and maximum *gmax* gradients are computed using the difference image acquired from equation (6):

$$gmax = \max\left(\nabla f_r\left(x,y\right)\right) = \max_{\Re}\left(\sum_{s=-r}^{r}\sum_{t=-r}^{r}\left(w(s,t)\cdot f_r\left(x+s,y+t\right)\right)\right),$$

$$g\min = \min\left(\nabla f_r\left(x,y\right)\right) = \min_{\Re}\left(\sum_{s=-r}^{r}\sum_{t=-r}^{r}\left(w(s,t)\cdot f_r\left(x+s,y+t\right)\right)\right),$$

$$(7)$$

where $f_r(x,y)$ is a pixel value taken from a difference image and $w(s,t)$ is a weighed matrix with the distance from its center value fixed for each cell. We also need to calculate the local limit gradients for every pixel for every *i-th* image in the series: and $lgmax_i(x,y) = \max(\nabla f_{ri}(x,y))$, and $lgmin_i(x,y) = \min(\nabla f_{ri}(x,y))$. Finally the conditions for depth map creation are described as:

```
if (gmax – lgmaxi) > a* (lgmin – gminj)
    Map(x,y) = i
else
    Map(x,y) = j
```

where `a` is a free parameter defining the gradient threshold level depending on the image characteristics.

The final image is generated using the depth map. For a given pixel position we select its final value from an image advised by the depth map. Finally, the new image has its levels automatically adjusted.

3. Results and discussion

Figure 7 shows an image series taken with different focus lengths, a reconstructed full focused image for this series and the depth map graphical representation. On this map there are clearly visible monochromatic fields that determine regions of the specific image in the series with the widest depth-of-field. Figure 8 presents another example of image series and reconstruction results. There is also a comparison between the reconstructed image using the presented algorithm and the image reconstruction obtained using the commercial product "HeliconFocus" [6] which has a very similar functionality but is a rather expensive product (30-250 depending on the version).

The Mean and the Standard Deviation of grey levels histogram defining the distribution of grey shades in the image were used to evaluate the sharpness degree of the examined image. Four sets of images were considered for both our algorithm (SemiVis) and HeliconFocus application. Table 1 shows the results for the first, middle and last image in the examined series (blurry images) and the results for HeliconFocus and SemiVis applications (reconstructed sharp image).

Fig. 7. An example of the whole series of images with the shallow depth-of-field problem with different focus length set (9 images at the top), depth map (bottom left) and reconstructed full focused image (bottom right)
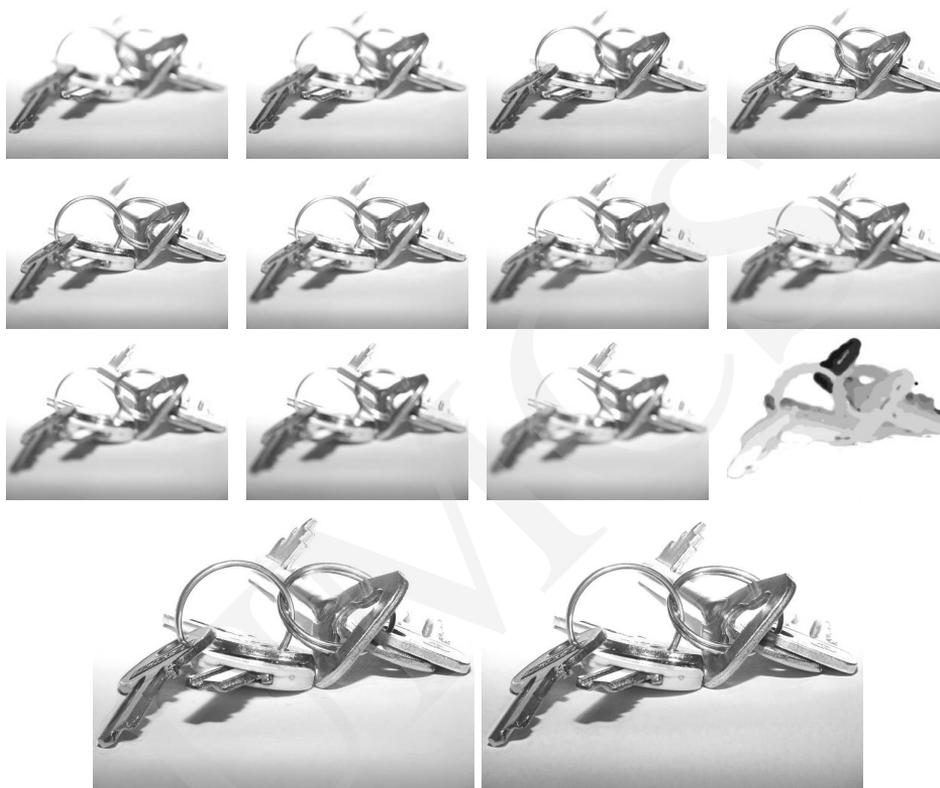
Fig. 8. A series of keys macro photograph taken with different focus length and the depth map for that series (12 top images), reconstructed image by out algorithm (bottom left) and reconstructed image by "HeliconFocus" (bottom right)

Table 1. Summary statistics of mean and standard deviation for four sets of images evaluated for SemiVis vs. HeliconFocus software.

Image	StdDev	Mean
keys00.jpg	45.98	212.05
keys07.jpg	49.90	208.09
keys15.jpg	36.62	223.11
keys-helicon.jpg	**51.39**	**206.92**
keys-semivis.jpg	**52.19**	**209.43**
text00.jpg	31.59	173.11
text06.jpg	40.14	171.95
text11.jpg	20.11	174.37
text-helicon.jpg	**51.69**	**164.28**
text-semivis.jpg	**54.67**	**165.70**
neckle00.jpg	55.04	101.35

neckle11.jpg	56.17	104.91
neckle22.jpg	55.69	107.26
neckle-helicon.jpg	**56.90**	**102.76**
neckle-semivis.jpg	**57.54**	**102.69**
flower00.jpg	49.92	119.99
flower05.jpg	53.54	115.51
flower10.jpg	53.55	117.71
flower-helicon.jpg	**56.10**	**113.59**
flower-semivis.jpg	**55.95**	**114.20**

The results show that the standard deviation is higher in a sharp image than in a blurry one, and the mean is slightly lower than the average mean in the whole series. A comparison between our algorithm and that used in the HeliconFocus application shows that both give images in a similar degree of sharpening with a little SemiVis advantage, but this advantage is in a standard error margin.

The presented algorithm was implemented in the c++ language with the Trolltech QT library as a module for the "Semivis" framework [7]. Using this application it is possible to create one completely focused image from several partially focused images by combining the focused areas. The program was designed for macro photography, but it can be also used with microphotography and hyperfocal landscape photography without any problems, due to the free parameters that the user can adjust depending on the type of processed images. There is also available a module that aligns images since photographed objects often change their size and position between the shots as well as automatically adjusting the brightness of the adjacent image. These functions are especially important in macro photography.

References

[1] Constant A., *Close-up Photography*, Butterworth-Heinemann, (2000).
[2] Shannon C.E., *A mathematical theory of communication*, Bell System Technical Journal, 27 (1948) 2790423 and 623.
[3] Studholme C., et al., *An overlap invariant entropy measure of 3D medical image alignment*, Pattern Recognition, 32(1) (1999) 71.
[4] Press W.H., Flannery B.P., Teukolsky S.A., Vetterling W.T., *Numerical Recipes in C*, Cambridge University Press, second edition, (1992).
[5] Gonzalez R.C, Woods R.E., *Digital image processing*, Addison-Wesley Publishing Company, Inc., (1992).
[6] http://helicon.com.ua – HeliconFocus main site.
[7] Denkowski M., Chlebiej M., Mikolajczak P., *The Development of the Cross-Platform Framework for Medical Image Processing*, Informatyka – Badania i Zastosowania, Kazimierz Dolny 9-11 Luty, 2005.